

The unified theory of n -dimensional complex and hypercomplex analytic signals

S.L. HAHN* and K.M. SNOPEK

Institute of Radioelectronics, Warsaw University of Technology, 15/19 Nowowiejska St., 00-665 Warszawa, Poland

Abstract. The paper is devoted to the theory of n -D complex and hypercomplex analytic signals with emphasis on the 3-dimensional (3-D) case. Their definitions are based on the proposed general n -D form of the Cauchy integral. The definitions are presented in signal- and frequency domains. The new notion of lower rank signals is introduced. It is shown that starting with the 3-D analytic hypercomplex signals and decreasing their rank by extending the support in the frequency-space to a so called space quadrant, we get a signal having the quaternionic structure. The advantage of this procedure is demonstrated in the context of the polar representation of 3-D hypercomplex signals. Some new reconstruction formulas are presented. Their validation has been confirmed using two 3-D test signals: a Gaussian one and a spherical one.

Key words: complex/hypercomplex analytic signal, hypercomplex Fourier transform, hypercomplex delta distribution.

1. Introduction

The theory of complex (CS) and hypercomplex (HS) signals is a subject of many publications involving mathematicians and engineers [1–12].

The theory of n -D CS with single-orthant spectra is presented in [9] and [10]. The evidence that these signals are boundary distributions of n -D analytic functions is given in [11]. This paper extends the evidence for HS which are boundary distributions of hypercomplex analytic functions. The case of $n=2$ has already been explored in [12] where the theory of 2-D quaternionic HS has been presented. It has been shown later in [13] that the polar representation of quaternionic signals can be derived starting with the polar representation of 2-D CS. Here, we present an attempt to find similar relations between polar representations of 3-D CS and HS. The organization of the paper is as follows.

In Sec. 2, we define a new hypercomplex Cauchy integral and show that both n -D CS and HS are boundary distributions of complex/hypercomplex analytic functions. In Sec. 3, selected algebras of basis vectors for 3-D octonionic signals are presented. The Secs. 4 and 5 are devoted to relationships between complex and hypercomplex 2-D and 3-D analytic signals. The Octonionic FT is introduced and the octonionic signal with a single-octant spectrum is defined. The Sec. 6 is devoted to the polar representation of 3-D analytic CS and HS. Some relations for the case 2-D are recalled and some new results for 3-D signals are presented. In the next Sec. 7 the hypothesis about the polar form of an octonionic signal is verified basing on numerical examples. The Sec. 8 is the overview of energy properties of analytic signals. The last Sec. 9 is the introduction to study of 4-D CS and HS.

2. The complex and hypercomplex multidimensional analytic functions defined by the Cauchy integral

Consider the n -D hypercomplex space C^n of hypercomplex variables: $z = (z_1, z_2, \dots, z_n)$: $z_k = x_k + y_k e_k$ where e_k are imaginary units (in the domain of complex numbers they are usually denoted as $z_k = x_k + j y_k$). The space C^n is a Cartesian product of complex planes C_k , $k = 1, 2, \dots, n$, that is, $C^n = C_1 \times C_2 \times \dots \times C_n$. We define a complex-valued n -D function $f(z)$, analytic (holomorphic) in the interior of a region $D^n = D_1 \times D_2 \times \dots \times D_n$, $D^n \subset C^n, D_k \subset C_k$.

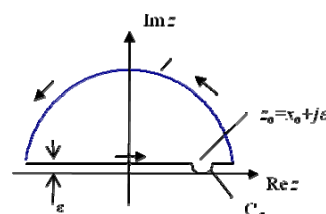


Fig. 1. The closed contour ∂D of integration in the complex plane ($n = 1$)

In [11], it has been shown that n -D analytic signals with single-orthant spectra are boundary distributions of n -D analytic functions represented by the n -D Cauchy integral. In this paper, we propose the unified representation of complex and hypercomplex analytic signals introducing the generalized form of the Cauchy integral:

$$f(z) = \frac{1}{(2\pi e_1)(2\pi e_1) \dots (2\pi e_n)} \oint_{\partial D_1} \dots \oint_{\partial D_n} \frac{f(\xi_1, \dots, \xi_n) d^n \xi}{(\xi_1 - z_1) \dots (\xi_n - z_n)}, \quad (1)$$

*e-mail: hahn@ire.pw.edu.pl

where ∂D_k are closed contours in D_k (see Fig. 1 for $n = 1$). For $n = 1$, inserting $e_1 = j$, $z_1 = z$ and $\partial D_1 = \partial D$ we obtain the well known Cauchy integral

$$f(z) = \frac{1}{2\pi j} \oint_{\partial D} \frac{f(\xi) d\xi}{\xi - z}. \quad (2)$$

In the complex case, all imaginary units in (1) are equal and usually denoted with j and any order of integration can be applied. In the general case, if $\{e_k\}$ form the basis of a non-commutative algebra, the order of integration should be defined. It can be shown by induction that if (1) is valid for $n - 1$, it is also valid for n variables [11]. Therefore, starting from (2) we can confirm the validity of (1).

It has been shown in [11] that the successive integration of the classical Cauchy integral yields the following equivalent two forms of the n -D analytic signal:

$$\psi_c(x) = \frac{1}{2^n} \prod_{k=1}^n (I_k \{u(x_k)\} + e_1 H_k \{u(x_k)\}), \quad (3)$$

$$\psi_c(x) = \frac{1}{2^n} u(x) * \prod_{k=1}^n \left[\delta(x_k) + e_1 \frac{1}{\pi x_k} \right], \quad (4)$$

where I_k is the 1-D identity operator w.r.t. x_k given by

$$I_k \{u(x_k)\} = u(x_k) * \delta(x_k) = u(x_k) \quad (5)$$

and H_k is the 1-D Hilbert transformation operator w.r.t. x_k :

$$H_k \{u(x_k)\} = u(x_k) * \frac{1}{\pi x_k} = v_k(x). \quad (6)$$

Let us note that using of the factor $1/2^n$ in (3) and (4) (in order to normalize the energy of a signal) is a matter of convention.

According to [11], the 1-D analytic signal $\psi(t) = u(t) + e_1 v(t)$ is a boundary distribution of the 1-D analytic function along the 0^+ side of the real axis of the $z = x + e_1 y$ plane and has the form

$$\psi(t) = I \{u\} + e_1 H \{u\} = u(t) * \left[\delta(t) + e_1 \frac{1}{\pi t} \right]. \quad (7)$$

For $n = 2$, we have

$$\psi(x_2, x_1) = I \{u\} - H \{u\} + e_1 (H_1 \{u\} + H_2 \{u\}), \quad (8)$$

that can be written as a product:

$$\psi(x_2, x_1) = (I_1 \{u\} + e_1 H_1 \{u\}) (I_2 \{u\} + e_1 H_2 \{u\}). \quad (9)$$

The straightforward generalization of (3) for n -D hypercomplex signals as boundary distributions of (1) is

$$\psi(x) = \prod_{i=1}^n (I_i \{u(x_i)\} + e_i H_i \{u(x_i)\}). \quad (10)$$

We also have

$$\psi(x) = u(x) * \Psi^\delta(x), \quad (11)$$

where

$$\Psi^\delta(x) = \prod_{i=1}^n [\delta(x_i) + e_i / \pi x_i] \quad (12)$$

is called the n -D hypercomplex delta distribution [14, 15]. Note that the signs of e_i in (12) are all positive. As it will explained in Sec. 4, it corresponds to the spectral support in the 1^{st} orthant of the frequency space. An appropriate change of signs defines spectral support in other orthants. The negative sign of a given e_i defines a boundary distribution at the 0^- side of the real axis in Fig. 1 and the integral contour included in the half-plane $\text{Im } z < 0$.

3. The choice of the algebra of basis vectors

The form of n -D analytic HS defined as boundary distributions of the analytic function (1) is not unique and depends on the algebra of basis vectors $\{e_1, e_2, \dots, e_n\}$. In this paper, we apply the Cayley-Dickson algebra [16, 17]. For $n = 3$, we have the non-commutative and non-associative algebra of octonions satisfying multiplication rules presented in Table 1¹. We have $e_i e_j = -e_j e_i$ and $e_i (e_j e_k) = -(e_i e_j) e_k$. Table 2 shows that each e_i has three different representations $e_i = e_j e_k$ ($-e_i = e_k e_j$).

Table 1
Cayley multiplication table, $n = 3$

\times	$\mathbf{1}$	e_1	e_2	e_3	e_4	e_5	e_6	e_7
$\mathbf{1}$	$\mathbf{1}$	e_1	e_2	e_3	e_4	e_5	e_6	e_7
e_1	e_1	-1	e_3	$-e_2$	e_5	$-e_4$	$-e_7$	e_6
e_2	e_2	$-e_3$	-1	e_1	e_6	e_7	$-e_4$	$-e_5$
e_3	e_3	e_2	$-e_1$	-1	e_7	$-e_6$	e_5	$-e_4$
e_4	e_4	$-e_5$	$-e_6$	$-e_7$	-1	e_1	e_2	e_3
e_5	e_5	e_4	$-e_7$	e_6	$-e_1$	-1	$-e_3$	e_2
e_6	e_6	e_7	e_4	$-e_5$	$-e_2$	e_3	-1	$-e_1$
e_7	e_7	$-e_6$	e_5	e_4	$-e_3$	$-e_2$	e_1	-1

Table 2
Products of imaginary units in the Cayley-Dickson algebra, $n = 3$

$e_1 = e_2 e_3 = e_4 e_5 = e_7 e_6$	$-e_1 = e_3 e_2 = e_5 e_4 = e_6 e_7$
$e_2 = e_3 e_1 = e_4 e_6 = e_5 e_7$	$-e_2 = e_1 e_3 = e_6 e_4 = e_7 e_5$
$e_3 = e_1 e_2 = e_4 e_7 = e_6 e_5$	$-e_3 = e_2 e_1 = e_7 e_4 = e_5 e_6$
$e_4 = e_5 e_1 = e_6 e_2 = e_7 e_3$	$-e_4 = e_1 e_5 = e_2 e_6 = e_3 e_7$
$e_5 = e_1 e_4 = e_3 e_6 = e_7 e_2$	$-e_5 = e_4 e_1 = e_6 e_3 = e_2 e_7$
$e_6 = e_1 e_7 = e_2 e_4 = e_5 e_3$	$-e_6 = e_7 e_1 = e_4 e_2 = e_3 e_5$
$e_7 = e_2 e_5 = e_3 e_4 = e_6 e_1$	$-e_7 = e_5 e_2 = e_4 e_3 = e_1 e_6$

The author of [18] defined n -D HS using the Clifford algebra with the basis formed by products of imaginary units: $\{e_{i_1} e_{i_2} \dots e_{i_k} : 1 \leq i_1 \leq \dots \leq i_k \leq n, 0 \leq k \leq n\}$. The Clifford algebra is non-commutative but associative with $e_i^2 = 1$ or $e_i^2 = -1$. It is usually denoted with $Cl_{p,q}(R)$ where p is the number of elements of the basis satisfying $e_i^2 = 1$ and q – the number of elements with $e_i^2 = -1$. So, $Cl_{0,1}(R)$ is the algebra of complex numbers, $Cl_{1,0}(R)$ – algebra of double numbers, $Cl_{0,2}(R)$ – algebra of quaternions and $Cl_{0,3}(R)$ – algebra of split-biquaternions [19]. The multiplication rules in $Cl_{0,3}(R)$ are presented in Tables 3 and 4 where $\omega = e_1 e_2 e_3$. Note that for $n = 1$ and $n = 2$, the sub-algebras of Tables 1 and 3 are the same. As a consequence, it will be shown

¹The Table 1, originally invented by Cayley is an example of 480 possible multiplication tables defined as cross-products of basis vectors [20, 21].

in Sec. 4 that definitions of Quaternionic Fourier transform (QFT) and Clifford FT coincide for $n = 1, 2$.

Table 3
Multiplication rules in $Cl_{0,3}(R)$

\times	1	e_1	e_2	e_3	e_1e_2	e_1e_3	e_2e_3	ω
1	1	e_1	e_2	e_3	e_1e_2	e_1e_3	e_2e_3	ω
e_1	e_1	-1	e_1e_2	e_1e_3	- e_2	- e_3	ω	- e_2e_3
e_2	e_2	- e_1e_2	-1	e_2e_3	e_1	- ω	- e_3	e_1e_3
e_3	e_3	- e_1e_3	- e_2e_3	-1	- ω	e_1	e_2	e_1e_2
e_1e_2	e_1e_2	e_2	- e_1	ω	-1	e_2e_3	- e_1e_3	- e_3
e_1e_3	e_1e_3	e_3	ω	- e_1	- e_2e_3	-1	e_1e_2	- e_2
e_2e_3	e_2e_3	- ω	e_3	- e_2	e_1e_3	- e_1e_2	-1	e_1
ω	ω	e_2e_3	- e_1e_3	- e_1e_2	e_3	e_2	- e_1	1

Table 4
Products of imaginary units in the Clifford algebra, $n = 3$

$e_1 = e_2(e_1e_2) = e_3(e_1e_3) = (e_2e_3)\omega$	$e_1 = (e_1e_2)e_2 = (e_1e_3)e_3 = \omega(e_2e_3)$
$e_2 = e_3(e_2e_3) = (e_1e_2)e_1 = \omega(e_1e_3)$	$e_2 = e_1(e_1e_2) = (e_2e_3)e_3 = (e_1e_3)\omega$
$e_3 = (e_1e_3)e_1 = (e_2e_3)e_2 = \omega(e_1e_2)$	$e_3 = e_1(e_1e_3) = e_2(e_2e_3) = (e_1e_2)\omega$
$e_1e_2 = e_1 \cdot e_2 = e_3\omega = (e_1e_3)(e_2e_3)$	$e_1e_2 = e_2 \cdot e_1 = \omega e_3 = (e_2e_3)(e_1e_3)$
$e_1e_3 = e_1 \cdot e_3 = e_2\omega = (e_2e_3)(e_1e_2)$	$e_1e_3 = e_3 \cdot e_1 = \omega e_2 = (e_1e_2)(e_2e_3)$
$e_2e_3 = e_2 \cdot e_3 = (e_1e_2)(e_1e_3) = \omega e_1$	$e_2e_3 = e_3 \cdot e_2 = (e_1e_3)(e_1e_2) = e_1\omega$
$\omega = e_1(e_2e_3) = (e_1e_2)e_3 = (e_1e_3)e_2$	$-\omega = (e_2e_3)e_1 = e_3(e_1e_2) = e_2(e_1e_3)$

4. Complex and hypercomplex Fourier transforms

As described in the next section, analytic signals can be alternatively defined using inverse Fourier transforms of their spectra. Let us define three basic FTs of a n -D real signal $u(\mathbf{x})$, $\mathbf{x} = (x_n, x_{n-1}, \dots, x_2, x_1)$ applied in this paper. The Fourier transformations define respectively complex/hypercomplex spectra: $U(\mathbf{f}), \mathbf{f} = (f_n, f_{n-1}, \dots, f_2, f_1)$.

4.1. The complex n -D FT. The n -D complex Fourier transform is given by the integral

$$U_c(\mathbf{f}) = \int_{R^n} u(\mathbf{x}) \prod_{i=1}^n \exp(-e_1 2\pi f_i x_i) d^n \mathbf{x} = \text{Re} + e_1 \text{Im} \quad (13)$$

and its inverse is

$$u(\mathbf{x}) = \int_{R^n} U_c(\mathbf{f}) \prod_{i=1}^n \exp(e_1 2\pi f_i x_i) d^n \mathbf{f}. \quad (14)$$

Note that the choice of the imaginary unit e_1 in (13)–(14) is arbitrary because there are two other options: e_2 and e_3 . However applying e_1 , we will see that definitions of the complex FT, Cayley-Dickson FT and Clifford FT coincide for $n = 1$.

4.2. Two hypercomplex Fourier transforms. There are many possible definitions of hypercomplex Fourier transforms dictated by the choice of the algebra of imaginary units $\{e_1, e_2, \dots, e_n\}$, as it has been mentioned in Sec. 3. In this paper, the dominant role plays the hypercomplex FT with imaginary units satisfying the multiplication rules of the Cayley-Dickson algebra (see Tables 1, 2) [15]:

$$U_{CD}(\mathbf{f}) = \int_{R^n} u(\mathbf{x}) \prod_{i=0}^{n-1} \exp(-e_2 i 2\pi f_{i+1} x_{i+1}) d^n \mathbf{x} \quad (15)$$

and its inverse

$$u(\mathbf{x}) = \int_{R^n} \left(\prod_{i=0}^{n-1} \exp(e_2^{n-i-1} 2\pi f_{n-i} x_{n-i}) \right) U_{CD}(\mathbf{f}) d^n \mathbf{f}. \quad (16)$$

Note that in (15), we apply in the exponent the following sequence of imaginary units: $e_1, e_2, e_4, e_8, \dots$. Differently, the sequence $e_1, e_2, e_3, e_4, \dots$ is applied in the Clifford Fourier transform defined by the integral

$$U_{Cl}(\mathbf{f}) = \int_{R^n} u(\mathbf{x}) \prod_{i=1}^n \exp(-e_i 2\pi f_i x_i) d^n \mathbf{x}. \quad (17)$$

This name is not unique since we can apply different Clifford algebras. Let us notice that for $n = 1$, the formulas (13), (15) and (17) define all the same 1-D complex FT:

$$U(f) = \int_R u(x) \exp(-e_1 2\pi f x) dx \quad \text{where } x = t \text{ denotes usually a time variable.}$$

For $n = 2$, (15) and (17) define the same Quaternionic Fourier Transform (QFT):

$$\text{QFT}(f_2, f_1) = \int_{R^2} u(x_2, x_1) e^{-e_1 2\pi f_1 x_1} e^{-e_2 2\pi f_2 x_2} dx_2 dx_1. \quad (18)$$

Its inverse is

$$u(x_2, x_1) = \int_{R^2} \text{QFT}(f_2, f_1) e^{e_1 2\pi f_1 x_1} e^{e_2 2\pi f_2 x_2} df_2 df_1. \quad (19)$$

Note that due to the non-commutativity of quaternions, the order of imaginary units in (17)–(18) is strictly determined and its change gives other definitions of hypercomplex FTs.

Next for $n = 3$, (15) and (16) define the so called Octonionic Fourier Transform (OFT) and its inverse:

$$\text{OFT}(f) = \int_{R^3} u(x) e^{-e_1 2\pi f_1 x_1} e^{-e_2 2\pi f_2 x_2} e^{-e_4 2\pi f_3 x_3} d^3 x, \quad (20)$$

$$u(x) = \int_{R^3} e^{e_4 2\pi f_3 x_3} e^{e_2 2\pi f_2 x_2} e^{e_1 2\pi f_1 x_1} \text{OFT}(f) d^3 f. \quad (21)$$

Again, the order of imaginary units in (20)–(21) is strictly defined and its change gives another definition of the OFT.

4.3. The comparison of the 3-D CFT with the OFT. Let us compare the 3-D FT and the OFT of a 3-D real signal $u(x_3, x_2, x_1)$ expressed as a union of eight terms (see Appendix A):

$$u(x_3, x_2, x_1) = u_{eee} + u_{eeo} + u_{oeo} + u_{ooo} + u_{ooe} + u_{oee} + u_{oeo} + u_{ooo}, \quad (22)$$

where the subscripts define even parity (e) and odd parity (o) w.r.t. variables (x_3, x_2, x_1) . Note that if e represents a binary “0” and o - a binary “1”, we get the binary sequence: 000, 001, 010, 011, 100, 101, 110, 111 of subscripts in (22). The insertion of (22) into (13) yields the 3-D Fourier spectrum

$$\begin{aligned}
 U(f_3, f_2, f_1) &= U_{eee} - U_{eoo} - U_{oeo} - U_{ooe} + \\
 &+ e_1(-U_{eoo} - U_{oeo} - U_{oeo} + U_{ooo}) = \\
 &= \text{Re}(f_3, f_2, f_1) + e_1 \text{Im}(f_3, f_2, f_1).
 \end{aligned}
 \tag{23}$$

The corresponding OFT of (22) is

$$\begin{aligned}
 \text{OFT}(f_3, f_2, f_1) &= U_{eee} - e_1 U_{eoo} - e_2 U_{oeo} + \\
 &+ e_3 U_{eoo} - e_4 U_{oeo} + e_5 U_{oeo} + e_6 U_{ooe} - e_7 U_{ooo}.
 \end{aligned}
 \tag{24}$$

Note also that 3-D signals symmetric w.r.t the origin, e.g. the zero-mean 3-D Gaussian signals (see Appendix B), have only the real spectrum ($\text{Im} = 0$). The imaginary part of (23) exists only if the symmetric signal is shifted to a new origin by x_{30} , x_{20} and x_{10} along the axes x_3 , x_2 and x_1 respectively. Due to the signal-domain shift property of the FT, the resulting spectrum is multiplied by $e^{-e_1 2\pi f_3 x_{30}} e^{-e_1 2\pi f_2 x_{20}} e^{-e_1 2\pi f_1 x_{10}}$. For symmetric signals, the Eq. (24) reduces to

$$\text{OFT}(f_3, f_2, f_1) = U_{eee} + e_3 U_{eoo} + e_5 U_{oeo} + e_6 U_{ooe}. \tag{25}$$

Both the complex and hypercomplex FT give exactly the same information about the frequency content of the n -D real signal. The choice of a method is a matter of convention or interpretation and is based on pure technical reasons.

4.4. Closed formulae enabling calculation of QFT and OFT starting with the CFT. A good evidence of the above statement is given by relations between the complex FT (13), the QFT (18) and OFT (20). The QFT can be calculated starting with the 2-D FT [6]:

$$\text{QFT}(f_2, f_1) = U_c(f_2, f_1) \frac{1 - e_3}{2} + U_c(-f_2, f_1) \frac{1 + e_3}{2}. \tag{26}$$

Similarly, we have shown (derivation in Appendix C) that the OFT is related to the 3-D FT by the following formula:

$$\begin{aligned}
 \text{OFT}(f_3, f_2, f_1) &= \frac{1}{4} U_c(f_3, f_2, f_1) (1 - e_3 - e_5 - e_6) + \\
 &+ \frac{1}{4} U_c(-f_3, f_2, f_1) (1 - e_3 + e_5 + e_6) + \\
 &+ \frac{1}{4} U_c(f_3, -f_2, f_1) (1 + e_3 - e_5 + e_6) + \\
 &+ \frac{1}{4} U_c(-f_3, -f_2, f_1) (1 + e_3 + e_5 - e_6).
 \end{aligned}
 \tag{27}$$

It should be pointed out that if in (13) the imaginary unit e_1 were replaced with e_2 or e_4 (see the remark following (14)), the formulas (26)–(27) would change. A similar formula exists also for the 3-D Clifford FT.

5. Complex and Hypercomplex 2-D and 3-D analytic signals

5.1. Frequency-domain definitions. The notion of the analytic signal with a single-orthant spectra has been introduced by Hahn [9] in 1992 and defined by the inverse FT (14) of a single-orthant spectrum. Later, the same author has shown that analytic signals with single-orthant spectra are boundary distributions of analytic functions [11]. Let us recall that the orthant is a half-axis in the 1-D case, a quadrant in 2-D, an

octant in 3-D, etc. The frequency-domain definition of the analytic signal with a single-orthant spectrum is

$$\psi(x) = \text{FT}^{-1} \{ \text{Spectrum} \times \text{Single-orthant Operator} \}, \tag{28}$$

$$\text{Single-orthant Operator} = \frac{1}{2^n} \prod_{i=1}^n (1 + \text{sgn} f_i). \tag{29}$$

Figure 2 presents the applied labelling of orthants in the 1-D, 2-D and 3-D frequency spaces (Notations: $s_i = \text{sgn} f_i$, $1 + s_i = 2 \cdot \mathbf{1}(f_i)$ where $\mathbf{1}(f_i)$ is a unit-step function). All orthants in the half-space $f_1 > 0$ are labelled with odd numbers.

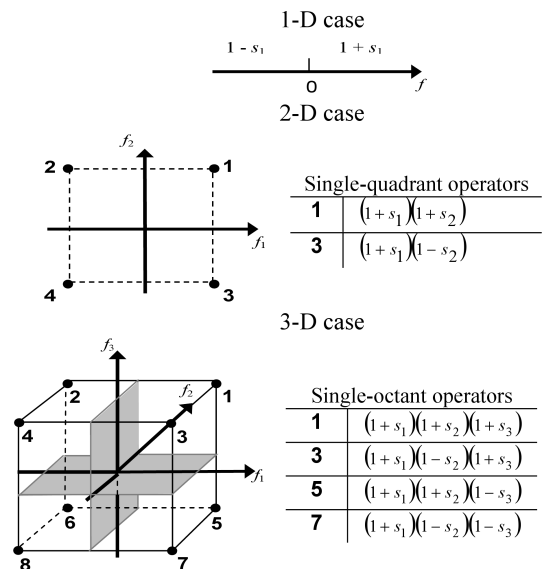


Fig. 2. Labelling of orthants in the 1-D, 2-D, 3-D frequency space and single-orthant operators

The factor $1/2^n$ in (29) can be omitted since it only normalizes the energy of a signal. So, if the energy of a real signal is E_u , the energy of the corresponding analytic signal is equal $2^n E_u$. We observe that a suitable change of signs of signum functions in (29) yields the spectrum in other orthants of the frequency space. Such a change corresponds to the change of signs of corresponding basis vectors in the Cauchy integral (1).

We see that the n -D frequency-space is divided into $N = 2^n$ orthants. Therefore, Eq. (28) defines 2^n different analytic signals. In consequence, due to the Hermitian symmetry of the Fourier transformation, a n -D real signal is represented by $N/2 = 2^{n-1}$ analytic signals. In this paper, we are focused on signals with spectra in the half-space $f_1 > 0$. As mentioned above, a 2-D real signal is equivalently represented by a single quaternionic analytic signal with a spectral support in the $1/4$ of the frequency-space. It is a consequence of the quaternionic Hermitian symmetry of the QFT described in [2] and [12]. In the hypercomplex 3-D case, the full information about the frequency content of a real signal is included in the $1/8$ of the (f_3, f_2, f_1) -space.

5.2. Signal-domain definition. Let us investigate details of Eq. (11). All analytic signals, complex or hypercomplex, are defined in the signal domain using the same real signal $u(x)$ and its total and partial Hilbert transforms as shown in (3) and (10). In the 2-D case, the convolutions

$$v_i(x_2, x_1) = u(x_2, x_1) * 1/(\pi x_i) \quad (30)$$

define respectively two 2-D partial Hilbert transforms w.r.t. x_1 and x_2 : v_1 and v_2 . The total 2-D Hilbert transform v is given by

$$v(x_2, x_1) = u(x_2, x_1) * * 1/(\pi^2 x_1 x_2). \quad (31)$$

In 3-D, we have three 1st-order partial Hilbert transforms v_i , $i = 1, 2, 3$:

$$v_i(x_3, x_2, x_1) = u(x_3, x_2, x_1) * 1/(\pi x_i) \quad (32)$$

and three 2nd-order partial Hilbert transforms v_{ij} , $i < j$, $i, j = 1, 2, 3$:

$$v_{ij}(x_3, x_2, x_1) = u(x_3, x_2, x_1) * * 1/(\pi^2 x_i x_j). \quad (33)$$

The total 3-D Hilbert transform is given by

$$v(x_3, x_2, x_1) = u(x_3, x_2, x_1) * * * 1/(\pi^3 x_1 x_2 x_3). \quad (34)$$

Complex analytic 2-D and 3-D signals. In the 2-D case, the half-space $f_1 > 0$ is divided into 2 quadrants as shown in Fig. 2. Therefore, we can define two analytic signals with spectra in quadrants No. 1 and 3 respectively [9, 10]. Using single-quadrant operators presented in Fig. 2 and applying the definition (28) we get:

$$\begin{aligned} \psi_1(x_2, x_1) &= F^{-1} \{(1 + s_1)(1 + s_2)U(f_2, f_1)\} = \\ &= u - v + e_1(v_1 + v_2), \end{aligned} \quad (35)$$

$$\begin{aligned} \psi_3(x_2, x_1) &= F^{-1} \{(1 + s_1)(1 - s_2)U(f_2, f_1)\} = \\ &= u + v + e_1(v_1 - v_2). \end{aligned} \quad (36)$$

Note that in (35) and (36) we omitted the normalization factor 1/4 in order to simplify the notation.

In the 3-D case, in the half-space $f_1 > 0$ we have 4 octants as shown in Fig. 2. Therefore for a real signal $u(x_3, x_2, x_1)$, we get four different complex analytic signals with spectral supports respectively in octants No. 1, 3, 5 and 7 (see Fig. 2):

$$\begin{aligned} \psi_1(x_3, x_2, x_1) &= \\ &= u - v_{12} - v_{13} - v_{23} + e_1(v_1 + v_2 + v_3 - v), \end{aligned} \quad (37)$$

$$\begin{aligned} \psi_3(x_3, x_2, x_1) &= \\ &= u + v_{12} - v_{13} + v_{23} + e_1(v_1 - v_2 + v_3 + v), \end{aligned} \quad (38)$$

$$\begin{aligned} \psi_5(x_3, x_2, x_1) &= \\ &= u - v_{12} + v_{13} + v_{23} + e_1(v_1 + v_2 - v_3 + v), \end{aligned} \quad (39)$$

$$\begin{aligned} \psi_7(x_3, x_2, x_1) &= \\ &= u + v_{12} + v_{13} - v_{23} + e_1(v_1 - v_2 - v_3 - v). \end{aligned} \quad (40)$$

Hypercomplex analytic 2-D and 3-D signals. The 2-D quaternionic analytic signals given by the inverse QFT (19) of the single-quadrant quaternionic spectra (in quadrants No. 1 and 3) are [2, 7]:

$$\begin{aligned} \psi_1^q(x_2, x_1) &= \\ &= \text{QFT}^{-1} \{(1 + s_1)(1 + s_2)U_q(f_2, f_1)\} = \\ &= u + e_1 v_1 + e_2 v_2 + e_3 v, \end{aligned} \quad (41)$$

$$\begin{aligned} \psi_3^q(x_2, x_1) &= \\ &= \text{QFT}^{-1} \{(1 + s_1)(1 - s_2)U_q(f_2, f_1)\} = \\ &= u + e_1 v_1 - e_2 v_2 - e_3 v. \end{aligned} \quad (42)$$

We see that (35), (36), (41) and (42) are defined exactly by the same functions.

The 3-D octonionic analytic signal with the 1st-octant spectral support is equal to the inverse OFT (21) of the 1st-octant octonionic spectrum:

$$\begin{aligned} \psi_1^o(x_3, x_2, x_1) &= \\ &= \text{OFT}^{-1} \{(1 + s_1)(1 + s_2)(1 + s_3)U_o(f_3, f_2, f_1)\} = \\ &= u + e_1 v_1 + e_2 v_2 + e_3 v_{12} + e_4 v_3 + e_5 v_{13} + e_6 v_{23} + e_7 v \end{aligned} \quad (43)$$

which can be expressed as a complex sum of two quaternionic signals:

$$\begin{aligned} \psi_1^o &= u + \underbrace{e_1 v_1 + e_2 v_2 + e_3 v_{12}}_{\psi_{q_1}} + \\ &+ \underbrace{(v_3 + e_1 v_{13} + e_2 v_{23} + e_3 v)}_{\psi_{q_2}} \cdot e_4 \end{aligned} \quad (44)$$

or as a union of four complex signals:

$$\begin{aligned} \psi_1^o &= \underbrace{u + e_1 v_1}_{\psi_{c_1}} + \underbrace{(v_2 + e_1 v_{12}) \cdot e_2}_{\psi_{c_2}} + \underbrace{(v_3 + e_1 v_{13}) \cdot e_4}_{\psi_{c_3}} \\ &+ \underbrace{(v_{23} + e_1 v)}_{\psi_{c_4}} \cdot e_6. \end{aligned} \quad (45)$$

Using the same reasoning, we get octonionic signals with spectral support in next octants labelled 3, 5 and 7 (the subscript indicates the octant number):

$$\psi_3^o = \psi_{c_1} - \psi_{c_2} e_2 + \psi_{c_3} e_4 - \psi_{c_4} e_6, \quad (46)$$

$$\psi_5^o = \psi_{c_1} + \psi_{c_2} e_2 - (\psi_{c_3} e_4 + \psi_{c_4} e_6), \quad (47)$$

$$\psi_7^o = \psi_{c_1} - \psi_{c_2} e_2 - (\psi_{c_3} e_4 - \psi_{c_4} e_6). \quad (48)$$

5.3. Notion of the ranking of complex/hypercomplex analytic signals. Let us explain the notion of ranking using the example of a 3-D signal. Let us assign to the four signals ψ_i^o , $i = 1, 3, 5, 7$ the highest rank $R = 3$. The idea is based on addition of two signals defined by (45) and (47) (respectively (46) and (48)) in such a way that its spectral support is doubled forming a so-called *space quadrant*. A space-quadrant is a union of two octants having a common plane in 3-D. We get

$$\begin{aligned} \psi_{1,5}^o(x_3, x_2, x_1) &= \frac{\psi_1^o + \psi_5^o}{2} = \\ &= \psi_{q_1} = u + e_1 v_1 + e_2 v_2 + e_3 v_{12} \end{aligned} \quad (49)$$

and

$$\begin{aligned} \psi_{3,7}^o(x_3, x_2, x_1) &= \frac{\psi_3^o + \psi_7^o}{2} \\ &= u + e_1 v_1 - (e_2 v_2 + e_3 v_{12}) \end{aligned} \quad (50)$$

i.e., two signals of rank $R = 2$ which have a quaternionic structure. The signal with the lowest rank $R = 1$ having a complex structure is

$$\psi_{1,3,5,7}^o(x_3, x_2, x_1) = \frac{\psi_1^o + \psi_3^o + \psi_5^o + \psi_7^o}{4} = u + e_1 v_1. \quad (51)$$

Its support is limited to the half-space $f_1 > 0$. The notion of ranking is useful especially in the context of the polar representation of signals. Let us note that the authors of [7] applied to (51) the name ‘‘partial analytic signal’’.

6. Polar representation of 3-D analytic signals

The polar representation of 1-D and 2-D signals is widely used in science and technology [25–27]. For a given real signal, there are many ways of defining a corresponding complex signal. This yields many possible definitions of its polar form. The polar representation of a real signal using its analytic form with single-orthant spectrum is unique. The evidence for 1-D signals is presented in [9, 10]. In order to define the polar form of octonionic signals, we need to recall some facts concerning the 2-D complex and quaternionic signals.

6.1. Polar representation of 2-D complex and quaternionic analytic signals. The 2-D analytic signals (35) and (36) can be written as

$$\psi_1(x_2, x_1) = A_1(x_2, x_1) e^{e_1 \varphi_1(x_2, x_1)}, \quad (52)$$

$$\psi_3(x_2, x_1) = A_3(x_2, x_1) e^{e_1 \varphi_3(x_2, x_1)}, \quad (53)$$

where the local amplitudes (squared) are

$$A_1^2(x_2, x_1) = u^2 + v_1^2 + v_2^2 + v^2 + 2(v_1 v_2 - uv), \quad (54)$$

$$A_3^2(x_2, x_1) = u^2 + v_1^2 + v_2^2 + v^2 - 2(v_1 v_2 - uv) \quad (55)$$

and local phase functions are given by

$$\tan \varphi_1(x_2, x_1) = \frac{v_1 + v_2}{u - v}, \quad (56)$$

$$\tan \varphi_3(x_2, x_1) = \frac{v_1 - v_2}{u + v}. \quad (57)$$

According to the definition introduced in [12], the 2-D quaternionic analytic signal (41) is defined in the following polar form:

$$\psi_q(x_2, x_1) = A_0 e^{e_1 \phi_1^q} e^{e_3 \phi_3^q} e^{e_2 \phi_2^q}, \quad (58)$$

where

$$A_0 = \sqrt{u^2 + v_1^2 + v_2^2 + v^2} \quad (59)$$

is the amplitude and $\phi_1^q, \phi_2^q, \phi_3^q$ are Euler angles representing three different phase functions. The Euler angles can be calculated from

$$\tan 2\phi_1^q = R_{32}/R_{22}, \quad (60)$$

$$\tan 2\phi_2^q = R_{13}/R_{11}, \quad (61)$$

$$\sin 2\phi_3^q = R_{12}/A_0^2, \quad (62)$$

where R_{ij} are elements of the Rodriguez matrix: $M(\psi_q) = (R_{ij})$ [2], i.e.,

$$R_{11} = u^2 + v_1^2 - v_2^2 - v^2, \quad R_{12} = 2(uv - v_1 v_2),$$

$$R_{13} = 2(v_1 v + uv_2), \quad R_{21} = 2(v_1 v_2 + uv),$$

$$R_{22} = u^2 - v_1^2 + v_2^2 - v^2, \quad R_{23} = 2(v_2 v - uv_1), \quad (63)$$

$$R_{31} = 2(v_1 v - uv_2), \quad R_{32} = 2(v_2 v + uv_1),$$

$$R_{33} = u^2 - v_1^2 - v_2^2 + v^2.$$

It has been proved in [13] that there are closed formulae enabling conversion from complex to quaternionic approach based on the equality: $\tan(\alpha \pm \beta) = \frac{\tan \alpha \pm \tan \beta}{1 \mp \tan \alpha \tan \beta}$. The full derivation is presented in the Appendix D. As shown in [13], we have

$$A_0^2 = \frac{A_1^2 + A_3^2}{2}, \quad (64)$$

$$\varphi_1 = \frac{1}{2}(\phi_1^q + \phi_2^q), \quad (65)$$

$$\varphi_3 = \frac{1}{2}(\phi_1^q - \phi_2^q), \quad (66)$$

$$\sin 2\phi_3^q = \frac{A_1^2 - A_3^2}{A_0^2}. \quad (67)$$

Reconstruction of a 2-D real signal. The real signal $u(x_2, x_1)$ can be reconstructed from its complex polar representation (52)–(53) (two amplitudes and two phase functions) using the formula [9]

$$u_{\text{rec}}(x_2, x_1) = \frac{A_1 \cos \varphi_1 + A_3 \cos \varphi_3}{2} \quad (68)$$

or from the quaternionic polar representation (58) (one amplitude and three phases) as follows:

$$\begin{aligned} u_{\text{rec}}(x_2, x_1) &= A_0 (\cos \phi_1^q \cos \phi_2^q \cos \phi_3^q - \\ &\quad - \sin \phi_1^q \sin \phi_2^q \sin \phi_3^q). \end{aligned} \quad (69)$$

6.2. Polar representation of 3-D complex and octonionic analytic signals. The 3-D complex signals (37)–(40) with single-octant spectra have the following polar forms

$$\psi_1(x_3, x_2, x_1) = A_1 e^{e_1 \varphi_1}, \quad (70)$$

$$\psi_3(x_3, x_2, x_1) = A_3 e^{e_1 \varphi_3}, \quad (71)$$

$$\psi_5(x_3, x_2, x_1) = A_5 e^{e_1 \varphi_5}, \quad (72)$$

$$\psi_7(x_3, x_2, x_1) = A_7 e^{e_1 \varphi_7}, \quad (73)$$

i.e., are defined by four amplitudes and four phase functions. Having in mind (52)–(53) and (70)–(73), we can now formulate a lemma:

Lemma. The total number of amplitude and phase functions of n -D complex/hypercomplex analytic signals is $M = 2^n$.

The above lemma is evident for complex analytic signals. Let us assume that it is also true for hypercomplex analytic signals. It has been already proven for $n = 2$ in [13] (complex case $2 + 2$, quaternionic: $1 + 3$). The case of 3-D hypercomplex analytic signals will be studied below.

The polar representation of the octonionic signal is actually only a partially solved problem. Having in mind the relations between octonions and the 7-dimensional cross-product [23], we are looking for its resolution in the exceptional Lie group G_2 – a subgroup of rotations in seven dimensions $SO(7)$ [24, 25].

Assuming that the polar form of an octonion can be the most probably derived starting with the four amplitudes and four phase functions of complex signals given by (70)–(73), we posit (with an indirect evidence) that such a derivation should be based on the formula of the tangent of a sum of four angles (in analogy to the 2-D case, as described in Appendix D). Such a procedure yields a formidable algebraic representation of the eventual 7-D extension of the Rodriguez matrix (see Appendix E). At present, we have been unable to derive such a matrix and received no advice from any experts working in the field. However, using deduction supported by the 2-D case and partly derivations, we arrived to the following polar representation of the octonionic analytic signal:

$$\begin{aligned} \psi_1^o(x_3, x_2, x_1) &= \\ &= A_0 e^{e_1 \phi_1^o} e^{e_3 \phi_3^o} e^{e_2 \phi_2^o} e^{e_7 \phi_7^o} e^{e_4 \phi_4^o} e^{e_6 \phi_6^o} e^{e_5 \phi_5^o}, \end{aligned} \quad (74)$$

where

$$A_0 = \sqrt{u^2 + v_1^2 + v_2^2 + v_{12}^2 + v_3^2 + v_{13}^2 + v_{23}^2 + v^2} \quad (75)$$

is the amplitude and $\phi_i^o, i = 1, 2, \dots, 7$ are seven phase functions. Let us explain the structure of (74). The order of exponents $e^{e_1 \phi_1^o} e^{e_3 \phi_3^o} e^{e_2 \phi_2^o}$ and $e^{e_4 \phi_4^o} e^{e_6 \phi_6^o} e^{e_5 \phi_5^o}$ is similar to the order used in (58). The central position of $e^{e_7 \phi_7^o}$ has been posited arbitrary. The seven phases $\phi_1^o, \dots, \phi_7^o$ form two groups: $\{\phi_1^o, \phi_2^o, \phi_4^o, \phi_5^o\}$ and $\{\phi_3^o, \phi_6^o, \phi_7^o\}$. The first group is defined as linear combinations of four phase functions $\varphi_i, i = 1, \dots, 4$, of 3-D complex analytic signals (see (70)–(73)):

$$\phi_1^o = (\varphi_1 + \varphi_3 + \varphi_5 + \varphi_7)/4, \quad (76)$$

$$\phi_2^o = (\varphi_1 + \varphi_3 - \varphi_5 - \varphi_7)/4, \quad (77)$$

$$\phi_4^o = (\varphi_1 - \varphi_3 + \varphi_5 - \varphi_7)/4, \quad (78)$$

$$\phi_5^o = (\varphi_1 - \varphi_3 - \varphi_5 + \varphi_7)/4. \quad (79)$$

In the case of separable 3-D signals, i.e., $u(x_3, x_2, x_1) = f_1(x_1) f_2(x_2) f_3(x_3)$, the corresponding complex signal is $\psi_1(x_3, x_2, x_1) = \psi_a(x_1) \psi_b(x_2) \psi_c(x_3)$ with $\psi_a(x_1) = A_a e^{e_1 \alpha_1}$, $\psi_b(x_2) = A_b e^{e_2 \alpha_2}$, $\psi_c(x_3) = A_c e^{e_3 \alpha_3}$. All four amplitudes are equal: $A_1 = A_3 = A_5 = A_7 = A_a A_b A_c$ and four phase functions are

$$\varphi_1 = \alpha_1 + \alpha_2 + \alpha_3, \quad (80)$$

$$\varphi_3 = \alpha_1 - \alpha_2 + \alpha_3, \quad (81)$$

$$\varphi_5 = \alpha_1 + \alpha_2 - \alpha_3, \quad (82)$$

$$\varphi_7 = \alpha_1 - \alpha_2 - \alpha_3. \quad (83)$$

The insertion of (80)–(83) into (76)–(79) yields $\phi_1^o = \alpha_1$, $\phi_2^o = \alpha_2$, $\phi_4^o = \alpha_3$, $\phi_5^o = 0$. In this case, we get identical polar forms of the 3-D complex and octonionic signals: $A_0 e^{e_1 \phi_1^o} e^{e_2 \phi_2^o} e^{e_4 \phi_4^o}$. Such a simplification is possible only if

the phase functions of the second group: $\phi_3^o, \phi_6^o, \phi_7^o$ have a similar structure as the phase functions of the 2-D quaternionic signal given by (67). They should be functions of four amplitudes A_1, A_3, A_5, A_7 and vanish if these amplitudes are equal. Having this in mind, we posit the following forms:

$$\sin(4\phi_3^o) = \frac{A_1^2 - A_3^2}{A_1^2 + A_3^2}, \quad (84)$$

$$\sin(4\phi_6^o) = \frac{A_5^2 - A_7^2}{A_5^2 + A_7^2}, \quad (85)$$

$$\sin(4\phi_7^o) = \frac{A_1^2 + A_3^2 - A_5^2 - A_7^2}{A_1^2 + A_3^2 + A_5^2 + A_7^2}. \quad (86)$$

1. Reconstruction of a 3-D real signal

The 3-D real signal can be reconstructed from its complex analytic signal (four amplitudes and four phase functions) by

$$u_{\text{rec}}(x_3, x_2, x_1) = \frac{A_1^c \cos \varphi_1^c + A_3^c \cos \varphi_3^c + A_5^c \cos \varphi_5^c + A_7^c \cos \varphi_7^c}{4}. \quad (87)$$

In the hypercomplex case, the polar form (74) yields the following reconstruction formula of the 3-D real signal $u(x_3, x_2, x_1)$:

$$\begin{aligned} u_{\text{rec}}(x_3, x_2, x_1) &= A_0 [c_1 c_2 c_3 c_4 c_5 c_6 c_7 + s_1 s_2 s_3 c_4 c_5 c_6 c_7 \\ &- s_1 c_2 c_3 s_4 s_5 c_6 c_7 + c_1 s_2 s_3 s_4 s_5 c_6 c_7 - s_1 s_2 c_3 s_4 c_5 s_6 c_7 \\ &+ s_1 c_2 s_3 s_4 c_5 s_6 c_7 - c_1 c_2 s_3 c_4 s_5 s_6 c_7 - s_1 s_2 c_3 c_4 s_5 s_6 c_7 \\ &+ c_1 c_2 s_3 s_4 c_5 c_6 s_7 + s_1 s_2 c_3 s_4 c_5 c_6 s_7 + c_1 s_2 c_3 c_4 s_5 c_6 s_7 \\ &- c_1 c_2 c_3 s_4 s_5 s_6 s_7 - s_1 s_2 s_3 s_4 s_5 s_6 s_7] \end{aligned} \quad (88)$$

with $c_i = \cos \phi_i^o$ and $s_i = \sin \phi_i^o$. For 3-D separable signals (87) and (88) are reduced to a common form

$$u_{\text{rec}}(x_3, x_2, x_1) = A_0 \cos \alpha_1 \cos \alpha_2 \cos \alpha_3. \quad (89)$$

Let us mention that (74) could not be defined using the Clifford 3-D analytic signal, since the amplitude (75) differs by the sign of v^2 . This is caused by the multiplication rule $\omega^2 = 1$ (see Table 3).

7. Verification of the polar form of octonionic analytic signals

Let us verify the polar form of the octonion analytic signal (79) using numerical calculations of the amplitude and seven phase functions of two test signals: the 3-D Gaussian signal (the most smooth one of all signals) and the signal in form of a sphere with a sharp edge. The verification compares the original signal $u(\mathbf{x})$ with the signal reconstructed using the amplitude and seven phase functions defined by (76)–(79) and (84)–(86) basing on cross-sections $u(x_3 = 0, x_2, x_1)$ and $u_{\text{rec}}(x_3 = 0, x_2, x_1)$. We proceeded as follows:

1. We calculated four amplitudes and four phase functions of complex analytic signals (70)–(73). The signal $u(\mathbf{x})$ and its seven Hilbert transforms are calculated using the inverse FT of their spectra. Note that due to the constraints of numerical calculations, it is not advisable to calculate the signal $u(\mathbf{x})$ directly from its representation in the signal

domain \mathbf{x} and the Hilbert transforms using the inverse FT of the spectra.

- In the next step we calculate the amplitude and seven phase functions using (76)–(79) and (84)–(86) and compare the reconstructed signal given by the formula (88) with the original signal $u(\mathbf{x})$.

Case 1. Non-separable Gaussian signal: $\sigma_1 = \sigma_2 = \sigma_3 = 0.5$ and $\rho_{12} = \rho_{13} = \rho_{23} = 0.7$.

The cross-section of the original signal $u(x_3 = 0, x_2, x_1)$ is shown in Fig. 3 and its reconstructed replica (88) $u_{rec}(x_3 = 0, x_2, x_1)$ in Fig. 4. Their difference illustrated in Fig. 5 is small but not negligible. We failed to find an alternative modification of phase angles (84)–(86) giving a smaller difference.

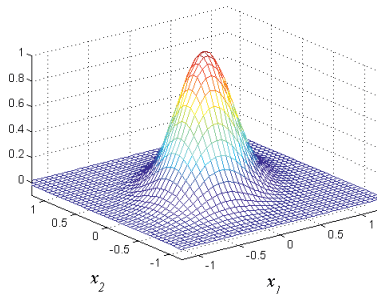


Fig. 3. Cross-section $u(x_3 = 0, x_2, x_1)$ of the real Gaussian 3-D non-separable signal

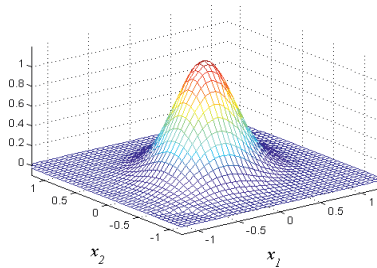


Fig. 4. The signal reconstructed using (88). It differs only slightly from the original signal of Fig. 3

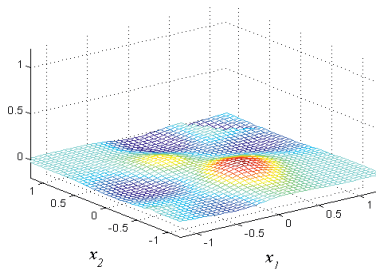


Fig. 5. The difference between the signal reconstructed using (68) and the original signal of Fig. 3

Case 2. A separable Gaussian signal: $\rho_{12} = \rho_{13} = \rho_{23} = 0$.

The difference of both cross-sections, as expected, equals zero. The case 2 validates (76)–(79) and (84)–(86). Let us have a comment on the non-separable case. We have two alternatives: Firstly, (84)–(86) could be improved and secondly, such an improvement is impossible. This dilemma could be solved only by theoretical derivation of (73).

Case 3. Non-separable Gaussian signal of Case 1. Comparison of cross-sections for quaternionic 3-D signal of rank 2. Here the reconstruction is perfect as shown in Fig. 6.

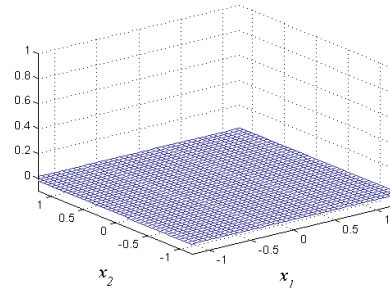


Fig. 6. The difference between the non-separable real 3-D Gaussian signal and its reconstructed versions defined by (49) (rank-2 hyper-complex) and (69) (complex). In both cases the reconstruction is perfect

Case 4. The original signal has the form of a sphere (see Appendix F). Its cross-section for $x_3 = 0$ is illustrated in Fig. 7. However in calculations, we used the signal derived by the inverse Fourier transform of the spectrum. Differently to the Gaussian case, this signal differs from the original one due to the Gibb's and edge effects. The corresponding cross-section is shown in Fig. 8 and the difference in Fig. 9. The cross-section $u_{rec}(x_3 = 0, x_2, x_1)$ of the signal reconstructed using (88) is shown in Fig. 10 and the difference in Fig. 11. We see that the difference is large only at the edges.

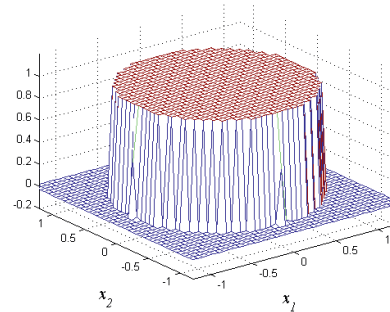


Fig. 7. The cross-section $u(x_3 = 0, x_2, x_1)$ of the sphere given by (F1)

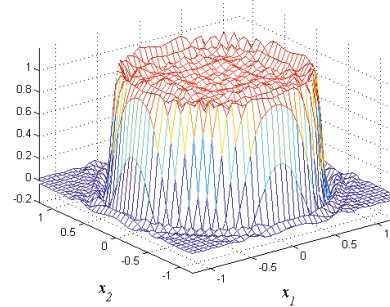


Fig. 8. The cross-section $u(x_3 = 0, x_2, x_1)$ obtained by the numerical calculation of the inverse Fourier transform of the spectrum given by (F2)

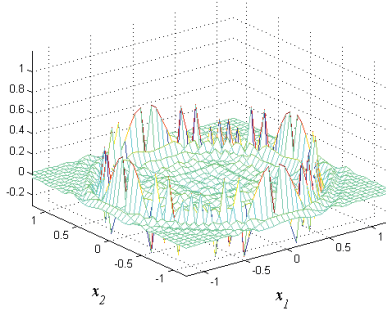


Fig. 9. The difference of cross-sections of the signal calculated in the signal domain (Fig. 7) and calculated using the inverse FT (Fig. 8)

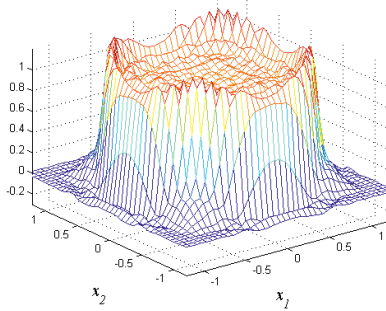


Fig. 10. The cross-section $u_{\text{rec}}(x_3 = 0, x_2, x_1)$ of the sphere reconstructed using Eq. (88)

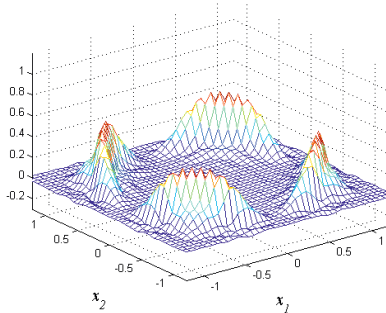


Fig. 11. The difference of cross-sections from Figs. 8 and 10

Case 5. We repeated the reconstruction of the sphere using the rank-2 quaternionic 3-D representation (49) and its polar form (58). Figure 12 shows the cross-section of the reconstructed signal and Fig. 13 the difference of Figs. 8 and 12. The error is negligible.

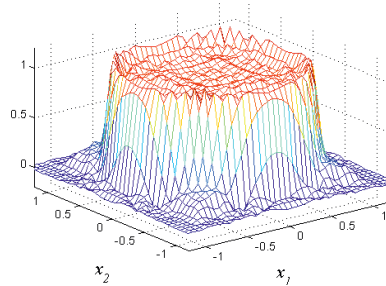


Fig. 12. The cross-section $u_{\text{rec}}(x_3 = 0, x_2, x_1)$ obtained from rank-2 octonionic signals (50)

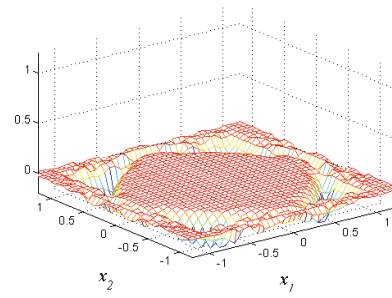


Fig. 13. The difference of cross-sections from Figs 8 and 12

8. Energies of signals with single-orthant spectra

The energies of signals with single-orthant spectra can be calculated either in signal- or in frequency domains. Here we present the frequency domain approach. It is well known that the complex spectrum defined by the FT (13) is redundant. Due to the Hermitian symmetry of FT, we have to consider only a half-space spectrum, in this paper a half-space $f_1 > 0$. The energy of a given signal is defined by the integral of the energy density over the volume V of a given orthant:

$$E_i = \int_V (\text{energy density}) dV, \quad (90)$$

e.g., in the half-space $f_1 > 0$, for orthants labelled 1, 3, 5, 7, ... (see Fig. 2).

The energies of complex and hypercomplex signals are different. Let us present examples for 2-D and 3-D signals. For convenience of presentation, let us consider signals with a real spectrum defined by (13) (e.g. zero-mean Gaussian signals).

8.1. Case 2-D.

$$U_1(f_2, f_1) = U_{ee} - U_{oo}, \quad (91)$$

$$U_3(-f_2, f_1) = U_{ee} + U_{oo}. \quad (92)$$

The energy densities are defined by U_1^2 and U_3^2 . Evidently, we have

$$E_1 = E_{ee} + E_{oo} - 2E_{eo}, \quad (93)$$

$$E_3 = E_{ee} + E_{oo} + 2E_{eo}, \quad (94)$$

i.e., the energies of signals with spectra in the 1st and 3rd quadrants differ by the amount of the mutual term $2E_{eo}$.

The authors of [12] have shown that the spectra of quaternionic 2-D signals have the property of quaternionic Hermitian symmetry. In our example we have

$$U_1^q(f_2, f_1) = U_{ee} - e_1 U_{oo}, \quad (95)$$

$$U_3^q(-f_2, f_1) = U_{ee} + e_1 U_{oo}. \quad (96)$$

Evidently, the energy densities are

$$U_1^q (U_1^q)^* = U_3^q (U_3^q)^* = U_{ee}^2 + U_{oo}^2 \quad (97)$$

so the energies in both quadrants are the same.

8.2. Case 3-D. For signals with a real spectrum we have

$$U_1(f_3, f_2, f_1) = U_{eee} - U_{eoo} - U_{oeo} - U_{ooe}, \quad (98)$$

$$U_3(f_3, -f_2, f_1) = U_{eee} + U_{eoo} - U_{oeo} + U_{ooe}, \quad (99)$$

$$U_5(-f_3, f_2, f_1) = U_{eee} - U_{eoo} + U_{oeo} + U_{ooe}, \quad (100)$$

$$U_7(-f_3, -f_2, f_1) = U_{eee} + U_{eoo} + U_{oeo} - U_{ooe}. \quad (101)$$

The energy densities in successive octants differ having the form

$$U_i^2 = U_{eee}^2 + U_{eoo}^2 + U_{oeo}^2 + U_{ooe}^2 + \text{Mutual terms}, \quad (102)$$

where mutual terms may be different in successive octants. In consequence, the energies E_1, E_3, E_5 and E_7 may differ.

For the hypercomplex octonic spectra:

$$U_1^o(f_3, f_2, f_1) = U_{eee} + e_3U_{eoo} + e_5U_{oeo} + e_6U_{ooe}, \quad (103)$$

$$U_3^o(f_3, -f_2, f_1) = U_{eee} - e_3U_{eoo} + e_5U_{oeo} - e_6U_{ooe}, \quad (104)$$

$$U_5^o(-f_3, f_2, f_1) = U_{eee} + e_3U_{eoo} - e_5U_{oeo} - e_6U_{ooe}, \quad (105)$$

$$U_7^o(-f_3, -f_2, f_1) = U_{eee} - e_3U_{eoo} - e_5U_{oeo} + e_6U_{ooe} \quad (106)$$

all energy densities in all octants are the same and equal

$$(U_i^o)^2 = U_{eee}^2 + U_{eoo}^2 + U_{oeo}^2 + U_{ooe}^2. \quad (107)$$

8.3. Rank-2 signals. Despite the fact that energies of all four rank-3 octonionic signals are the same, the energies of rank-2 signals with space-quadrant spectral support are different and depend on the orientation of space quadrants (two possibilities). For the orientation along the f_3 axis, we have

$$U_{1,5}^o = \frac{U_1^o + U_5^o}{2} = U_{eee} + e_3U_{eoo}, \quad (108)$$

$$U_{3,7}^o = \frac{U_3^o + U_7^o}{2} = U_{eee} - e_3U_{eoo} \quad (109)$$

and for the orientation along the f_2 axis

$$U_{1,3}^o = \frac{U_1^o + U_3^o}{2} = U_{eee} + e_5U_{oeo}, \quad (110)$$

$$U_{5,7}^o = \frac{U_5^o + U_7^o}{2} = U_{eee} - e_5U_{oeo}. \quad (111)$$

For these two pairs of conjugate rank-2 signals, the energy densities may be different and then yield different energies. Note the fact that though we assumed for complex signals a real spectrum, the corresponding spectra of hypercomplex signals are hypercomplex.

9. 4-D analytic signals

The general formula (28) defining the n -D complex signals with single-orthant spectra can be used to derive eight 4-D analytic signals with spectra in 8 octants of the half-space $f_1 > 0$ (labelled 1, 3, 5, 7, 9, 11, 13, 15), representing a 4-D real signal $u(x_4, x_3, x_2, x_1)$. Such a signal has in general 16 terms of different parity w.r.t. variables x_4, x_3, x_2, x_1 . We have

$$u(x) = u_{eeee} + u_{eeeo} + \dots + u_{oooe} + u_{oooo}, \quad (112)$$

where subscripts represent successive binary numbers (according to the convention: e - "0", o - "1"). The 4-D FT yields the following complex spectrum

$$U(f) = U_{eeee} - U_{eeoo} - U_{eooe} - U_{eoeo} - U_{ooee} - U_{ooeo} - U_{oooo} - e_1(U_{eeeo} + U_{eeoe} + U_{eoee} - U_{eooo} + U_{oeee} + U_{oeoo} + U_{ooeo} + U_{oooe}) \quad (113)$$

Applying (15) for $n = 4$ and the multiplication rules of the algebra of sedenions (see Table 4), we obtain the corresponding hypercomplex spectrum:

$$U_{CD}(f) = U_{eeee} - e_1U_{eeeo} - e_2U_{eeoe} + e_3U_{eooo} - e_4U_{eoee} + e_5U_{eoeo} + e_6U_{eooe} - e_7U_{eooo} - e_8U_{oeee} + e_9U_{oeeo} + e_{10}U_{oeoe} - e_{11}U_{oeoo} + e_{12}U_{ooee} - e_{13}U_{ooeo} - e_{14}U_{oooe} + e_{15}U_{oooo}. \quad (114)$$

Table 4
Cayley multiplication table, $n = 4$

\times	1	e_1	e_2	e_3	e_4	e_5	e_6	e_7	e_8	e_9	e_{10}	e_{11}	e_{12}	e_{13}	e_{14}	e_{15}
1	1	e_1	e_2	e_3	e_4	e_5	e_6	e_7	e_8	e_9	e_{10}	e_{11}	e_{12}	e_{13}	e_{14}	e_{15}
e_1	e_1	-1	e_3	$-e_2$	e_5	$-e_4$	$-e_7$	e_6	e_9	$-e_8$	$-e_{11}$	e_{10}	$-e_{13}$	e_{12}	e_{15}	$-e_{14}$
e_2	e_2	$-e_3$	-1	e_1	e_6	e_7	$-e_4$	$-e_5$	e_{10}	e_{11}	$-e_8$	$-e_9$	$-e_{14}$	$-e_{15}$	e_{12}	e_{13}
e_3	e_3	e_2	$-e_1$	-1	e_7	$-e_6$	e_5	$-e_4$	e_{11}	$-e_{10}$	e_9	$-e_8$	$-e_{15}$	e_{14}	$-e_{13}$	e_{12}
e_4	e_4	$-e_5$	$-e_6$	$-e_7$	-1	e_1	e_2	e_3	e_{12}	e_{13}	e_{14}	e_{15}	$-e_8$	$-e_9$	$-e_{10}$	$-e_{11}$
e_5	e_5	e_4	$-e_7$	e_6	$-e_1$	-1	$-e_3$	e_2	e_{13}	$-e_{12}$	e_{15}	$-e_{14}$	e_9	$-e_8$	e_{11}	$-e_{10}$
e_6	e_6	e_7	e_4	$-e_5$	$-e_2$	e_3	-1	$-e_1$	e_{14}	$-e_{15}$	$-e_{12}$	e_{13}	e_{10}	$-e_{11}$	$-e_8$	e_9
e_7	e_7	$-e_6$	e_5	e_4	$-e_3$	$-e_2$	e_1	-1	e_{15}	e_{14}	$-e_{13}$	$-e_{12}$	e_{11}	e_{10}	$-e_9$	$-e_8$
e_8	e_8	$-e_9$	$-e_{10}$	$-e_{11}$	$-e_{12}$	$-e_{13}$	$-e_{14}$	$-e_{15}$	-1	e_1	e_2	e_3	e_4	e_5	e_6	e_7
e_9	e_9	e_8	$-e_{11}$	e_{10}	$-e_{13}$	e_{12}	e_{15}	$-e_{14}$	$-e_1$	-1	$-e_3$	e_2	$-e_5$	e_4	e_7	$-e_6$
e_{10}	e_{10}	e_{11}	e_8	$-e_9$	$-e_{14}$	$-e_{15}$	e_{12}	e_{13}	$-e_2$	e_3	-1	$-e_1$	$-e_6$	$-e_7$	e_4	e_5
e_{11}	e_{11}	$-e_{10}$	e_9	e_8	$-e_{15}$	e_{14}	$-e_{13}$	e_{12}	$-e_3$	$-e_2$	e_1	-1	$-e_7$	e_6	$-e_5$	e_4
e_{12}	e_{12}	e_{13}	e_{14}	e_{15}	e_8	$-e_9$	$-e_{10}$	$-e_{11}$	$-e_4$	e_5	e_6	e_7	-1	$-e_1$	$-e_2$	$-e_3$
e_{13}	e_{13}	$-e_{12}$	e_{15}	$-e_{14}$	e_9	e_8	e_{11}	$-e_{10}$	$-e_5$	$-e_4$	e_7	$-e_6$	e_1	-1	e_3	$-e_2$
e_{14}	e_{14}	$-e_{15}$	$-e_{12}$	e_{13}	e_{10}	$-e_{11}$	e_8	e_9	$-e_6$	$-e_7$	$-e_4$	e_5	e_2	$-e_3$	-1	e_1
e_{15}	e_{15}	e_{14}	$-e_{13}$	$-e_{12}$	e_{11}	e_{10}	$-e_9$	e_8	$-e_7$	e_6	$-e_5$	$-e_4$	e_3	e_2	$-e_1$	-1

The inverse FT (27) with eight different single-orthant operators yields 8 different complex analytic signals. Let us present only two of them: ψ_1 and ψ_9 :

$$\psi_1 = u - v_{12} - v_{13} - v_{14} - v_{23} - v_{24} - v_{34} + v + e_1(v_1 + v_2 + v_3 + v_4 - v_{123} - v_{124} - v_{134} - v_{234}), \quad (115)$$

$$\psi_9 = u - v_{12} - v_{13} + v_{14} - v_{23} + v_{24} + v_{34} - v + e_1(v_1 + v_2 + v_3 - v_4 - v_{123} + v_{124} + v_{134} + v_{234}). \quad (116)$$

The inverse hypercomplex FT (15) yields the following sedenionic signals:

$$\psi_1^s = u + e_1v_1 + e_2v_2 + e_3v_{12} + e_4v_3 + e_5v_{13} + e_6v_{23} + e_7v_{123} + e_8v_4 + e_9v_{14} + e_{10}v_{24} + e_{11}v_{124} + e_{12}v_{34} + e_{13}v_{134} + e_{14}v_{234} + e_{15}v, \quad (117)$$

$$\psi_9^s = u + e_1v_1 + e_2v_2 + e_3v_{12} + e_4v_3 + e_5v_{13} + e_6v_{23} + e_7v_{123} - e_8v_4 - e_9v_{14} - e_{10}v_{24} - e_{11}v_{124} - e_{12}v_{34} - e_{13}v_{134} - e_{14}v_{234} - e_{15}v. \quad (118)$$

Let us rewrite signals (115)–(118) as unions of eight complex signals. We have

$$\psi_1 = (u + e_1v_1) + (-v_{12} + e_1v_2) + (-v_{13} + e_1v_3) + (-v_{23} - e_1v_{123}) + (-v_{14} + e_1v_4) + (-v_{24} - e_1v_{124}) + (-v_{34} - e_1v_{134}) + (v - e_1v_{234}), \quad (119)$$

$$\psi_9 = (u + e_1v_1) + (-v_{12} + e_1v_2) + (-v_{13} + e_1v_3) + (-v_{23} - e_1v_{123}) + (v_{14} - e_1v_4) + (v_{24} + e_1v_{124}) + (v_{34} + e_1v_{134}) + (-v + e_1v_{234}), \quad (120)$$

$$\psi_1^s = (u + e_1v_1) + (v_2 + e_1v_{12}) e_2 + (v_3 + e_1v_{13}) e_4 + (v_{23} + e_1v_{123}) e_6 + (v_4 + e_1v_{14}) e_8 + (v_{24} + e_1v_{124}) e_{10} + (v_{34} + e_1v_{134}) e_{12} + (v_{234} + e_1v) e_{14}, \quad (121)$$

$$\psi_9^s = (u + e_1v_1) + (v_2 + e_1v_{12}) e_2 + (v_3 + e_1v_{13}) e_4 + (v_{23} + e_1v_{123}) e_6 - (v_4 + e_1v_{14}) e_8 - (v_{24} + e_1v_{124}) e_{10} - (v_{34} + e_1v_{134}) e_{12} - (v_{234} + e_1v) e_{14}. \quad (122)$$

The sedenionic signals ψ_1^s and ψ_9^s can be equivalently represented as unions of two octonionic signals

$$\psi_1^s = (u + e_1v_1 + e_2v_2 + e_3v_{12} + e_4v_3 + e_5v_{13} + e_6v_{23} + e_7v_{123}) + (v_4 + e_1v_{14} + e_2v_{24} + e_3v_{124} + e_4v_{34} + e_5v_{134} + e_6v_{234} + e_7v) e_8, \quad (123)$$

$$\psi_9^s = (u + e_1v_1 + e_2v_2 + e_3v_{12} + e_4v_3 + e_5v_{13} + e_6v_{23} + e_7v_{123}) - (v_4 + e_1v_{14} + e_2v_{24} + e_3v_{124} + e_4v_{34} + e_5v_{134} + e_6v_{234} + e_7v) e_8. \quad (124)$$

It is known [9, 10] that the polar representation of eight 4-D analytic complex signals defines 8 amplitudes and 8 phase functions. We have not tried to find the polar representation of

a sedenionic signal. Most probably, it would be very complicated or even impossible. However, the polar form can be derived for rank-3 signals. Signals ψ_1, \dots, ψ_{15} and $\psi_1^s, \dots, \psi_{15}^s$ have all the rank 4. The hypercomplex signal of rank 3 is

$$\psi_{1,9}^s = \frac{\psi_1^s + \psi_9^s}{2} = u + e_1v_1 + e_2v_2 + e_3v_{12} + e_4v_3 + e_5v_{13} + e_6v_{23} + e_7v_{123} \quad (125)$$

and has exactly the same form as the octonionic signal (45). Therefore, the procedure of calculating of a single amplitude and seven phase functions in (74) can be applied to (125). The difference is that here we deal with 4-D functions instead of 3-D.

10. Conclusions

The presented generalization of the theory of complex/hypercomplex signals can be summarized as follows:

1. The n -D CS and HS with single-orthant spectra are boundary distributions of complex/hypercomplex signals of n -D complex/hypercomplex analytic functions defined by the generalized Cauchy integral (1). The definition of the hypercomplex analytic function is not unique. It depends on the choice of the algebra of basis vectors e_i . This paper has shown some advantages of applying of the Cayley-Dickson algebra for the case $n \geq 3$.
2. The n -D CS/HS with single-orthant spectra have the common form of a convolution of the real signal $u(\mathbf{x})$ with the complex/hypercomplex delta distribution.
3. In the frequency domain, the CS/HS are defined by the inverse complex/hypercomplex FT of a single-orthant spectrum.
4. The choice between the complex or hypercomplex representation is a matter of convenience in derivations and interpretations. For example, the laws of electromagnetism can be described using complex or hypercomplex representation [28, 29].
5. We defined the notion of lower rank complex/hypercomplex analytic signals. For example, 3-D signals have the rank $R = 3$. The addition of two signals with single octant spectra produces a rank-2 signal with a space quadrant spectral support.
6. Each step in the derivation of a lower rank signal halves the number of terms of the analytic signal with no change of its dimensions. For example, the rank of a sedenionic signal is $R = 4$. The signal with $R = 3$ is a 4-D octonionic one, with $R = 2$ – a 4-D quaternionic one and with $R = 1$ – a 4-D complex signal.
7. We deduced (partly derived) the polar representation of the octonionic analytic signal. Numerical calculations using two test signals, a 3-D Gaussian and a sphere, validated this formula with a difference between the original and reconstructed signals of the order lower than 10%. However, the reconstruction using a rank-2 signal has been perfect. As well, the reconstruction is perfect for a rank-3 separable Gaussian signal. The formal derivation of the polar form of an octonion is still an unsolved problem.

8. As regards possible applications, we should look for them in the domain of HS in general or in the domain of HS having single-orthant spectra. We have found in many mathematical and physical publications some applications of quaternions and octonions and partly sedenions. Namely, the quaternions are used with success in color image processing and computer graphics. However, we have not come across any applications of analytic signals presented in this paper. Therefore, the perspectives of this work include further research on the applications of analytic complex and hypercomplex n -D signals.

Appendix A

Decomposition of a 3-D real signal into even-odd parts

A 3-D real signal $u(x_3, x_2, x_1)$ may be resolved into a sum of eight terms

$$u(x_3, x_2, x_1) = u_{eee} + u_{eoo} + u_{oeo} + u_{oee} + u_{oeo} + u_{ooe} + u_{ooo}, \quad (\text{A1})$$

where

$$u_{eee}(\cdot) = 1/16 \{u(x_3, x_2, x_1) + u(x_3, x_2, -x_1) + u(x_3, -x_2, x_1) + u(x_3, -x_2, -x_1) + u(-x_3, x_2, x_1) + u(-x_3, x_2, -x_1) + u(-x_3, -x_2, x_1) + u(-x_3, -x_2, -x_1)\}, \quad (\text{A2})$$

$$u_{eoo}(\cdot) = 1/16 \{u(x_3, x_2, x_1) - u(x_3, x_2, -x_1) + u(x_3, -x_2, x_1) - u(x_3, -x_2, -x_1) + u(-x_3, x_2, x_1) - u(-x_3, x_2, -x_1) + u(-x_3, -x_2, x_1) - u(-x_3, -x_2, -x_1)\}, \quad (\text{A3})$$

$$u_{oeo}(\cdot) = 1/16 \{u(x_3, x_2, x_1) + u(x_3, x_2, -x_1) - u(x_3, -x_2, x_1) - u(x_3, -x_2, -x_1) + u(-x_3, x_2, x_1) + u(-x_3, x_2, -x_1) - u(-x_3, -x_2, x_1) - u(-x_3, -x_2, -x_1)\}, \quad (\text{A4})$$

$$u_{ooo}(\cdot) = 1/16 \{u(x_3, x_2, x_1) - u(x_3, x_2, -x_1) - u(x_3, -x_2, x_1) + u(x_3, -x_2, -x_1) + u(-x_3, x_2, x_1) - u(-x_3, x_2, -x_1) - u(-x_3, -x_2, x_1) + u(-x_3, -x_2, -x_1)\}, \quad (\text{A5})$$

$$u_{oeo}(\cdot) = 1/16 \{u(x_3, x_2, x_1) + u(x_3, x_2, -x_1) + u(x_3, -x_2, x_1) + u(x_3, -x_2, -x_1) - u(-x_3, x_2, x_1) - u(-x_3, x_2, -x_1) - u(-x_3, -x_2, x_1) - u(-x_3, -x_2, -x_1)\}, \quad (\text{A6})$$

$$u_{ooe}(\cdot) = 1/16 \{u(x_3, x_2, x_1) - u(x_3, x_2, -x_1) + u(x_3, -x_2, x_1) - u(x_3, -x_2, -x_1) - u(-x_3, x_2, x_1) + u(-x_3, x_2, -x_1) - u(-x_3, -x_2, x_1) + u(-x_3, -x_2, -x_1)\}, \quad (\text{A7})$$

$$u_{ooo}(\cdot) = 1/16 \{u(x_3, x_2, x_1) + u(x_3, x_2, -x_1) - u(x_3, -x_2, x_1) - u(x_3, -x_2, -x_1) - u(-x_3, x_2, x_1) - u(-x_3, x_2, -x_1) + u(-x_3, -x_2, x_1) + u(-x_3, -x_2, -x_1)\}, \quad (\text{A8})$$

$$u_{ooo}(\cdot) = 1/16 \{u(x_3, x_2, x_1) - u(x_3, x_2, -x_1) - u(x_3, -x_2, x_1) + u(x_3, -x_2, -x_1) - u(-x_3, x_2, x_1) + u(-x_3, x_2, -x_1) + u(-x_3, -x_2, x_1) - u(-x_3, -x_2, -x_1)\}. \quad (\text{A9})$$

Appendix B

The 3-D Gaussian signal

The 3-D Gaussian signal is defined by

$$u(x_3, x_2, x_1) = (2\pi)^{-3/2} |M|^{-1/2} \exp \left\{ \frac{-1}{2|M|} \sum_{i,j=1}^3 |M_{ij}| x_i x_j \right\}, \quad (\text{B1})$$

where

$$|M| = \sigma_1^2 \sigma_2^2 \sigma_3^2 (1 + 2\rho_{12}\rho_{23}\rho_{13} - \rho_{12}^2 - \rho_{23}^2 - \rho_{13}^2),$$

$$|M_{11}| = (1 - \rho_{23}^2) \sigma_2^2 \sigma_3^2,$$

$$|M_{22}| = (1 - \rho_{13}^2) \sigma_1^2 \sigma_3^2,$$

$$|M_{33}| = (1 - \rho_{12}^2) \sigma_1^2 \sigma_2^2,$$

$$|M_{12}| = |M_{21}| = \sigma_1 \sigma_2 \sigma_3^2 (\rho_{23}\rho_{13} - \rho_{12}),$$

$$|M_{23}| = |M_{32}| = \sigma_1^2 \sigma_2 \sigma_3 (\rho_{12}\rho_{13} - \rho_{23})$$

and

$$|M_{13}| = |M_{31}| = \sigma_1 \sigma_2^2 \sigma_3 (\rho_{12}\rho_{23} - \rho_{13}).$$

The parameters σ_i^2 , $i = 1, 2, 3$ are called variances and ρ_{ij} , $i, j = 1, 2, 3, i \neq j$ are cross-correlation factors. If all $\rho_{ij} = 0$, we have a 3-D separable Gaussian signal. The Fourier spectrum $U(\omega_3, \omega_2, \omega_1)$, $\omega_i = 2\pi f_i$ of (B1) is

$$U(\omega_3, \omega_2, \omega_1) = \exp \left[-\frac{1}{2} (\omega_1^2 \sigma_1^2 + \omega_2^2 \sigma_2^2 + \omega_3^2 \sigma_3^2) \right] \cdot \exp \left[-(\omega_1 \omega_2 \rho_{12} \sigma_1 \sigma_2 + \omega_1 \omega_3 \rho_{13} \sigma_1 \sigma_3 + \omega_2 \omega_3 \rho_{23} \sigma_2 \sigma_3) \right]. \quad (\text{B2})$$

Appendix C

Derivation of the formula (27) relating 3-D FT and OFT

A. Formula relating the 3-D FT and the OFT

Let us recall the definition of the 3-D FT given by (13):

$$U(f_3, f_2, f_1) = \int_{R^3} u(\mathbf{x}) e^{-e_1 \alpha_1} e^{-e_1 \alpha_2} e^{-e_1 \alpha_3} d^3 \mathbf{x}, \quad (\text{C1})$$

where $\alpha_1 = 2\pi f_1 x_1$, $\alpha_2 = 2\pi f_2 x_2$, $\alpha_3 = 2\pi f_3 x_3$, $\alpha_3 = 2\pi f_3 x_3$ and $\mathbf{x} = (x_3, x_2, x_1)$. Let us calculate the sum

$$\frac{1}{2} [U(f_3, f_2, f_1) + U(-f_3, f_2, f_1)] = \int_{R^3} u(\mathbf{x}) e^{-e_1 \alpha_1} e^{-e_1 \alpha_2} (\cos \alpha_3) d^3 \mathbf{x} \quad (\text{C2})$$

and the difference

$$\frac{1}{2} [U(f_3, f_2, f_1) - U(-f_3, f_2, f_1)] = \int_{R^3} u(\mathbf{x}) e^{-e_1 \alpha_1} e^{-e_1 \alpha_2} (-e_1 \sin \alpha_3) d^3 \mathbf{x}. \quad (\text{C3})$$

Multiplying (C3) from the right by $(-e_5)$ and applying the multiplication rules from Table 1, we get

$$\begin{aligned} & \frac{1}{2} [U(f_3, f_2, f_1) - U(-f_3, f_2, f_1)] (-e_5) = \\ & = \int_{R^3} u(x) e^{-e_1 \alpha_1} e^{-e_1 \alpha_2} (-e_4 \sin \alpha_3) d^3 x. \end{aligned} \quad (C4)$$

Now adding (C2) and (C4) we obtain

$$\begin{aligned} & \frac{1}{2} U(f_3, f_2, f_1) (1 - e_5) + \\ & + \frac{1}{2} U(-f_3, f_2, f_1) (1 + e_5) = \\ & = \int_{R^3} u(x) e^{-e_1 \alpha_1} e^{-e_1 \alpha_2} e^{-e_4 \alpha_3} d^3 x. \end{aligned} \quad (C5)$$

To simplify the notation, let us introduce

$$\begin{aligned} V(f_3, f_2, f_1) &= \frac{1}{2} U(f_3, f_2, f_1) (1 - e_5) + \\ & + \frac{1}{2} U(-f_3, f_2, f_1) (1 + e_5) \end{aligned} \quad (C6)$$

and calculate once again two sums

$$\begin{aligned} & \frac{1}{2} [V(f_3, f_2, f_1) + V(f_3, -f_2, f_1)] = \\ & = \int_{R^3} u(x) e^{-e_1 \alpha_1} (\cos \alpha_2) e^{-e_4 \alpha_3} d^3 x, \end{aligned} \quad (C7)$$

$$\begin{aligned} & \frac{1}{2} [V(f_3, f_2, f_1) - V(f_3, -f_2, f_1)] = \\ & = \int_{R^3} u(x) e^{-e_1 \alpha_1} (-e_1 \sin \alpha_2) e^{-e_4 \alpha_3} d^3 x. \end{aligned} \quad (C8)$$

We notice in (C8) that the multiplication of $e^{-e_1 \alpha_1} (-e_1 \sin \alpha_2) e^{-e_4 \alpha_3}$ from the right by $(-e_3)$ is equivalent to $e^{e_1 \alpha_1} (e_1 e_3 \sin \alpha_2) e^{e_4 \alpha_3}$, and in consequence we obtain

$$\begin{aligned} & \frac{1}{2} [V(f_3, f_2, f_1) - V(f_3, -f_2, f_1)] e_3 = \\ & = \int_{R^3} u(x) e^{-e_1 \alpha_1} (-e_2 \sin \alpha_2) e^{e_4 \alpha_3} d^3 x. \end{aligned} \quad (C9)$$

Now, we add (C7) and (C9):

$$\begin{aligned} & \frac{1}{2} [V(f_3, f_2, f_1) + V(f_3, -f_2, f_1)] + \\ & + \frac{1}{2} [V(f_3, f_2, f_1) - V(f_3, -f_2, f_1)] e_3 = \\ & = \int_{R^3} u(x) e^{-e_1 \alpha_1} e^{-e_2 \alpha_2} e^{-e_4 \alpha_3} d^3 x. \end{aligned} \quad (C10)$$

Finally, from (C6) and (C10) we get the formula (27).

$$\begin{aligned} \text{OFT}(f_3, f_2, f_1) &= \\ &= \frac{1}{4} \{ U_c(f_3, f_2, f_1) (1 - e_5) + \\ & + U_c(-f_3, f_2, f_1) (1 + e_5) + \\ & + U_c(f_3, -f_2, f_1) (1 - e_5) + \\ & + U_c(-f_3, -f_2, f_1) (1 + e_5) \} + \\ & + \frac{1}{4} e_3 \{ U_c(f_3, f_2, -f_1) (1 - e_5) + \\ & + U_c(-f_3, f_2, -f_1) (1 + e_5) - \\ & - U_c(f_3, -f_2, -f_1) (1 - e_5) - \\ & - U_c(-f_3, -f_2, -f_1) (1 + e_5) \}. \end{aligned} \quad (C11)$$

Appendix D

Relations between 2-D analytic quaternionic and complex signals

Let us recall the phase functions of the analytic 2-D CS given by (56) and (57): $\tan \varphi_1(x_2, x_1) = (v_1 + v_2)/(u - v)$, $\tan \varphi_3(x_2, x_1) = (v_1 - v_2)/(u + v)$. The addition of (56) and (57) yields

$$\begin{aligned} \tan \varphi_1 + \tan \varphi_3 &= \frac{v_1 + v_2}{u - v} + \frac{v_1 - v_2}{u + v} = \\ &= \frac{2(v_1 u + v_2 v)}{u^2 - v^2} \end{aligned} \quad (D1)$$

and the subtraction

$$\begin{aligned} \tan \varphi_1 - \tan \varphi_3 &= \frac{v_1 + v_2}{u - v} - \frac{v_1 - v_2}{u + v} = \\ &= \frac{2(v_1 v + v_2 u)}{u^2 - v^2}. \end{aligned} \quad (D2)$$

From (60)–(62) it is known that the quaternionic phase functions $\phi_1^q, \phi_2^q, \phi_3^q$ are defined by

$$\tan 2\phi_1^q = \frac{2(v_2 v + u v_1)}{u^2 - v_1^2 + v_2^2 - v^2}, \quad (D3)$$

$$\tan 2\phi_2^q = \frac{2(v_1 v + u v_2)}{u^2 + v_1^2 - v_2^2 - v^2}, \quad (D4)$$

$$\sin 2\phi_3^q = \frac{2(uv - v_1 v_2)}{u^2 + v_1^2 + v_2^2 + v^2}. \quad (D5)$$

Introducing (D1) into (D3) we get

$$\begin{aligned} \tan 2\phi_1^q &= \frac{2(v_2 v + u v_1)}{u^2 - v_1^2 + v_2^2 - v^2} = \\ &= \frac{(\tan \varphi_1 + \tan \varphi_3) (u^2 - v^2)}{(u^2 - v^2) \left(1 - \frac{v_1^2 - v_2^2}{u^2 - v^2} \right)} = \\ &= \frac{\tan \varphi_1 + \tan \varphi_3}{1 - \frac{(v_1 + v_2)(v_1 - v_2)}{u - v} \frac{v_1 - v_2}{u + v}} = \\ &= \frac{\tan \varphi_1 + \tan \varphi_3}{1 - \tan \varphi_1 \tan \varphi_3}. \end{aligned} \quad (D6)$$

In (D6) we recognize:

$$\tan(\alpha + \beta) = \frac{\tan \alpha + \tan \beta}{1 - \tan \alpha \tan \beta}$$

and finally we get

$$2\phi_1^q = \varphi_1 + \varphi_3. \quad (D7)$$

Analogously, from (D2) and (D4) we have

$$\begin{aligned} \tan 2\phi_2^q &= \frac{\tan \varphi_1 - \tan \varphi_3}{1 - \frac{(v_1 + v_2)(v_1 - v_2)}{u - v} \frac{(v_1 - v_2)}{u + v}} = \\ &= \frac{\tan \varphi_1 - \tan \varphi_3}{1 + \tan \varphi_1 \tan \varphi_3} \end{aligned} \quad (D8)$$

and $2\phi_2^q = \varphi_1 - \varphi_3$.

Formulas (D7) and (D9) confirm relations (65) and (66): $\varphi_1 = \frac{1}{2}(\phi_1^q + \phi_2^q)$ and $\varphi_3 = \frac{1}{2}(\phi_1^q - \phi_2^q)$. The relation (D5) is trivial to prove by adding and subtracting (54) and (55). Using (59), we have

$$A_1^2 + A_3^2 = 2(u^2 + v_1^2 + v_2^2 + v^2) = 2A_0^2, \quad (D10)$$

$$A_1^2 - A_3^2 = 2(uv - v_1v_2) \quad (D11)$$

which prove the relation (D5).

Appendix E

Formidable algebraic representation of the tangent of a sum of four angles defined by the polar form of 3-D complex analytic signals

Consider the Eq. (76) written here again

$$\phi_1^o = (\varphi_1 + \varphi_3 + \varphi_5 + \varphi_7)/4. \quad (E1)$$

The four angles are defined by the polar form of four 3-D complex analytic signals given by (36)–(39). We have

$$\tan \varphi_1 = \frac{v_1 + v_2 + v_3 - v}{u - v_{12} - v_{13} - v_{23}} = \frac{N_1}{D_1}, \quad (E2)$$

$$\tan \varphi_3 = \frac{v_1 + v_2 - v_3 + v}{u - v_{12} + v_{13} + v_{23}} = \frac{N_3}{D_3}, \quad (E3)$$

$$\tan \varphi_5 = \frac{v_1 - v_2 + v_3 + v}{u + v_{12} - v_{13} + v_{23}} = \frac{N_5}{D_5}, \quad (E4)$$

$$\tan \varphi_7 = \frac{v_1 + v_2 + v_3 - v}{u - v_{12} - v_{13} - v_{23}} = \frac{N_7}{D_7}. \quad (E5)$$

The tangent of a sum of four angles is

$$\begin{aligned} \tan(\varphi_1 + \varphi_3 + \varphi_5 + \varphi_7) &= \\ &= \frac{\frac{\tan \varphi_1 + \tan \varphi_3}{1 - \tan \varphi_1 \tan \varphi_3} + \frac{\tan \varphi_5 + \tan \varphi_7}{1 - \tan \varphi_5 \tan \varphi_7}}{1 - \frac{\tan \varphi_1 + \tan \varphi_3}{1 - \tan \varphi_1 \tan \varphi_3} \cdot \frac{\tan \varphi_5 + \tan \varphi_7}{1 - \tan \varphi_5 \tan \varphi_7}}. \end{aligned} \quad (E6)$$

The insertion of (E2)–(E5) into (E6) yields after arrangement of terms a formidable algebraic expression in the form of a quotient of a nominator and denominator each being a sum of a big number of terms, each term in the form of a

product of four terms defined by nominators and denominators in (E2) to (E5). This shows how complicated could be the eventual matrix representation of the seven phase angles in (75).

Appendix F

The sphere and its 3-D spectrum

The sphere is a spherically symmetric function

$$u(r) = 0.5 - 0.5 \operatorname{sgn}(r - r_1). \quad (F1)$$

Its Fourier transform is

$$U(\omega) = \frac{4\pi}{\rho^3} [\sin(r_1\rho) - r_1\rho \cos(r_1\rho)], \quad (F2)$$

where $\rho = \|\omega\|$ [30].

REFERENCES

- [1] S.J. Sangwine, "Fourier transforms of colour images using quaternion or hypercomplex numbers", *Electron. Lett.* 32 (21), 1979–1980 (1996).
- [2] T. Bülow, "Hypercomplex spectral signal representation for the processing and analysis of images", in: *Bericht* No. 99–3, Institut für Informatik und Praktische Mathematik, Christian-Albrechts-Universität, Kiel, 1999.
- [3] T.A. Ell and S.J. Sangwine, "Hypercomplex Fourier transforms of color images", *IEEE Trans. Image Processing* 16 (1), 22–35 (2007).
- [4] D.S. Alexiadis and G.D. Sergiadis, "Estimation of motions in color image sequences using hypercomplex Fourier transforms", *IEEE Trans. Image Processing* 18 (1), 168–187 (2009).
- [5] S.J. Sangwine and T.A. Ell, "Color image filters based on hypercomplex convolution", *IEEE Proc. Vis. Image Signal Process.* 147 (2), 89–93 (2000).
- [6] S.-C. Pei, J. H. Chang, and J.-J. Ding, "Commutative reduced biquaternions and their Fourier transform for signal and image processing applications", *IEEE Trans. Signal Process.* 52 (7), 2012–2031 (2004).
- [7] T. Bülow, M. Felsberg, and G. Sommer, *Non-Commutative Hypercomplex Fourier Transforms of Multidimensional Signals, Geometric Computing with Clifford Algebra*, G. Sommer, ed., Springer-Verlag, Berlin, 2001.
- [8] A.K. Kwaśniewski, "Glimpses of the octonions and quaternions history and today's applications in quantum physics", *ArXiv e-prints*, http://aps.arxiv.org/PS_cache/arxiv/pdf/0803/0803.0119v1.pdf (2008).
- [9] S.L. Hahn, "Multidimensional complex signals with single-orthant spectra", *Proc. IEEE* 80 (8), 1287–1300 (1992).
- [10] S.L. Hahn, *Hilbert Transforms in Signal Processing*, Artech House Inc., Norwood, 1996.
- [11] S.L. Hahn, "Complex signals with single-orthant spectra as boundary distributions of multidimensional analytic functions", *Bull. Pol. Ac.: Tech.* 2 (2), 155–161 (2003).
- [12] T. Bülow and G. Sommer, "The hypercomplex signal – a novel extension of the analytic signal to the multidimensional case", *IEEE Trans. Signal Processing* 49 (11), 2844–2852 (2001).
- [13] S.L. Hahn and K.M. Snopek, "Comparison of properties of analytic, quaternionic and monogenic 2-D signals", *WSEAS Trans. Computers* 3 (3), 602–611 (2004).

- [14] S.L. Hahn, "The n-dimensional complex delta distribution", *IEEE Trans. Signal Proc.* 44, 1833–1837 (1996).
- [15] K.M. Snopek, "New hypercomplex analytic signals and Fourier transforms in Cayley-Dickson algebras", *Electronics and Telecommunications Q.* 55 (3), 403–415 (2009).
- [16] J.H. Conway and R.K. Guy, *Cayley Numbers. The Book of Numbers*, Springer-Verlag, New York, 1996.
- [17] P.R. Girard, *Quaternions, Clifford Algebras and Relativistic Physics*, Springer, Berlin, 2007.
- [18] T.A. Ell, "Hypercomplex spectral transforms", *Ph.D. Dissertation*, Univ. Minnesota, Minneapolis, 1992.
- [19] G. Sommer, *Geometric Computing with Clifford Algebras*, Springer-Verlag, Berlin, 2001.
- [20] W.S. Massey, "Cross products of vectors in higher dimensional Euclidean spaces", *Amer. Math. Monthly* 90 (10), 697–701 (1983).
- [21] E. Darpo, "Vector product algebras", *Bull. London Math. Soc.* 41, 898–902 (2009).
- [22] Z.S. Veličković and V.D. Pavlović, "Complex analytic signals applied on time delay estimation", *Facta Universitatis, Series: Physics, Chemistry and Technology* 6 (1), 11–28 (2008).
- [23] A.H. Ansari and K. Alamdar, "Reduction of the pole of magnetic anomalies using analytic signal", *World Appl. Sc. J.* 7 (4), 405–409 (2009).
- [24] M. Beiki, "Analytic signals of gravity gradient tensor and their application to estimate source location", *Geophysics* 75 (6), 159–174, (2010).
- [25] B. Boashash, "Estimating and interpreting the instantaneous frequency of a signal. Part I: Fundamentals", *Proc. IEEE* 80 (4), 520–538 (1992).
- [26] B. Boashash, "Estimating and interpreting the instantaneous frequency of a signal. Part II: Algorithms and applications", *Proc. IEEE* 80 (4), 539–568 (1992).
- [27] B.C. Lovell, R.C. Williamson, and B. Boashash, "The relationship between instantaneous frequency and time-frequency representations", *IEEE Trans. Signal Process.* 41 (3), 1458–1461 (1993).
- [28] T. Tolan, K. Özdaş, and M. Tanişli, "Reformulation of electromagnetism with octonions", *Il Nuovo Cimento* 121B (1), 43–55 (2006).
- [29] V.L. Mironov and S.V. Mironov, "Octonic representation of electromagnetic field equations", *J. Math. Physics* 50 (012901), 1–10 (2009).
- [30] The derivation of (F2) is delivered to us by Prof. K. Howell.